Electronic Supplementary Information

Symmetrically pumped charges with high confinement stiffness for boosted performance in wave energy harvesting

Huijing Qiu,[ab] Weizhi Song,[b] Zichao Deng,[bd] Zhong Lin Wang*[b] and Liang Xu*[abc]

[a] Center on Nanoenergy Research, Institute of Science and Technology for Carbon Peak & Neutrality; Key Laboratory of Blue Energy and Systems Integration (Guangxi University), Education Department of Guangxi Zhuang Autonomous Region; School of Physical Science & Technology, Guangxi University, Nanning, 530004, P. R. China.

[b] Beijing Institute of Nanoenergy and Nanosystems, Chinese Academy of Sciences, Beijing, 101400, P. R. China.

[c] School of Nanoscience and Engineering, University of Chinese Academy of Sciences, Beijing, 100049, P. R. China.

[d] Key Laboratory of Advanced Marine Materials; Key Laboratory of Marine Environmental Corrosion and Bio-fouling, Institute of Oceanology, Chinese Academy of Sciences, Qingdao, 266071, P. R. China.

* Corresponding authors: Liang Xu (e-mail: xuliang@binn.cas.cn), Zhong Lin Wang (e-mail: zhong.wang@mse.gatech.edu).

Content

Supplementary Figures:

Supplementary Movies:

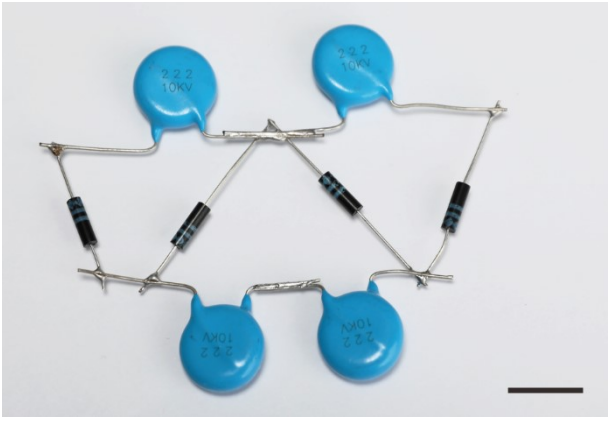

Fig. S1 Photograph of the voltage-multiplying circuit (VMC). Scale bar, 1.5 cm.

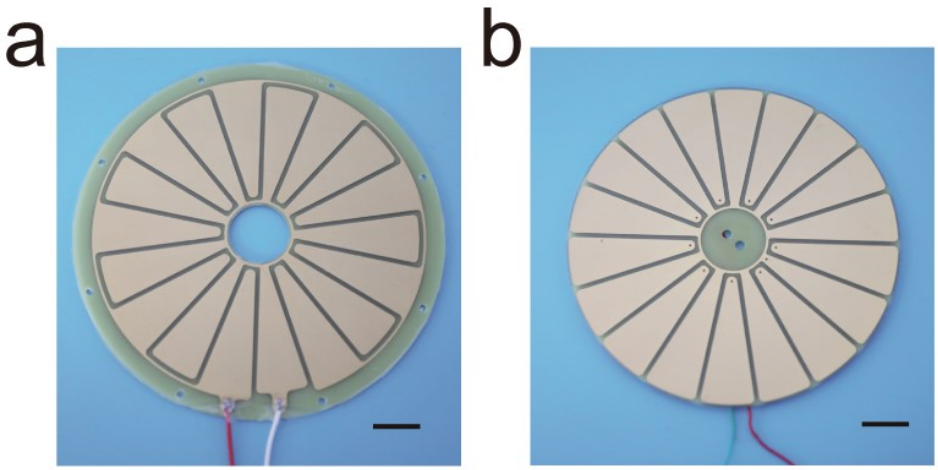

Fig. S2 Photographs of stator disk (a) and rotator disk (b). Scale bar, 2 cm.

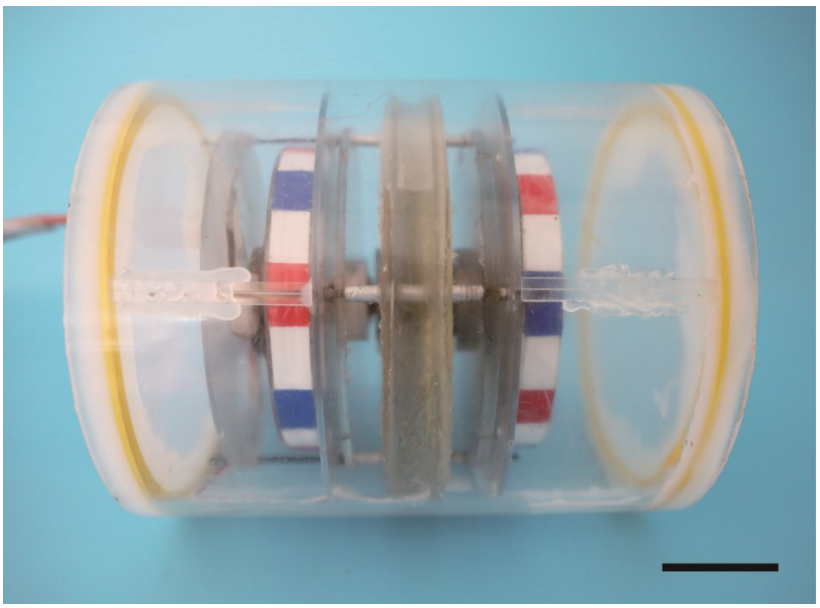

Fig. S3 Photograph of the as-fabricated device. Scale bar, 4 cm.

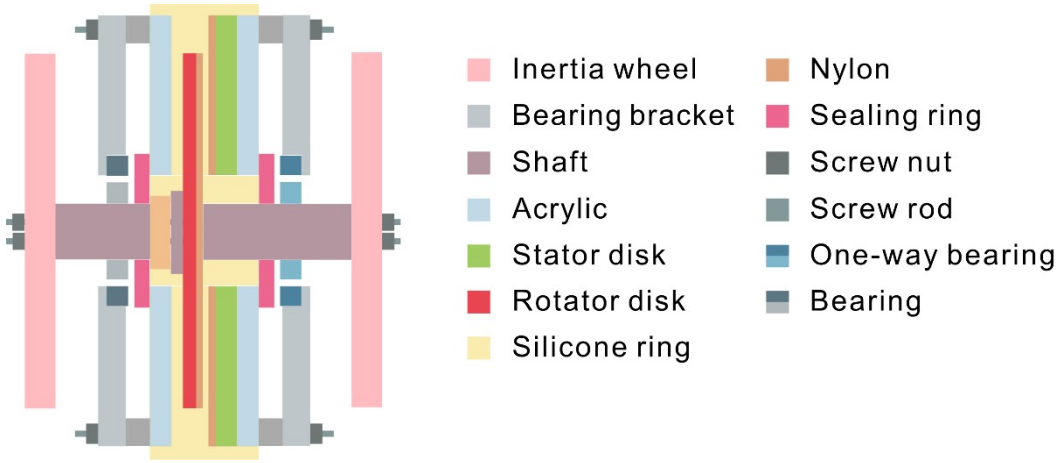

Fig. S4 Schematic side view of the device.

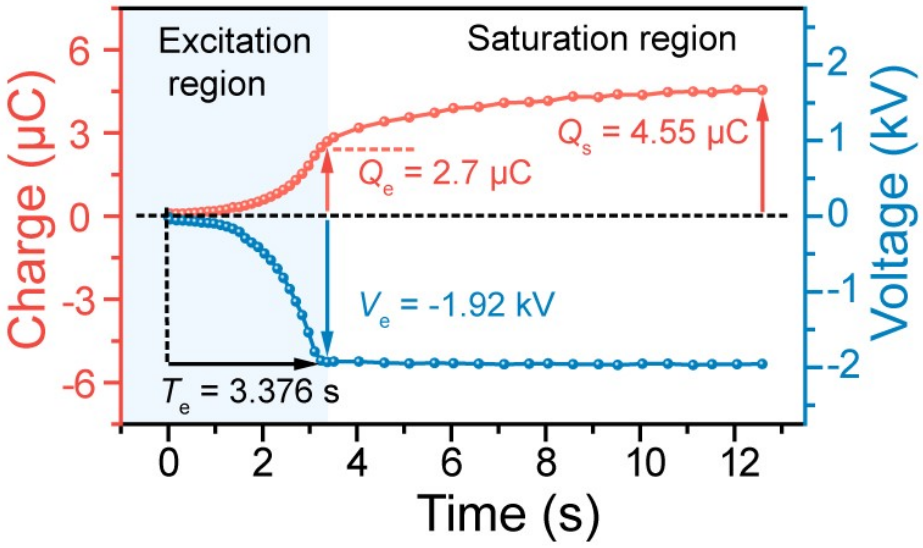

Fig. S5 Typical charge output and voltage of negative confinement electrode (CE) with a 2 kV Zener diode.

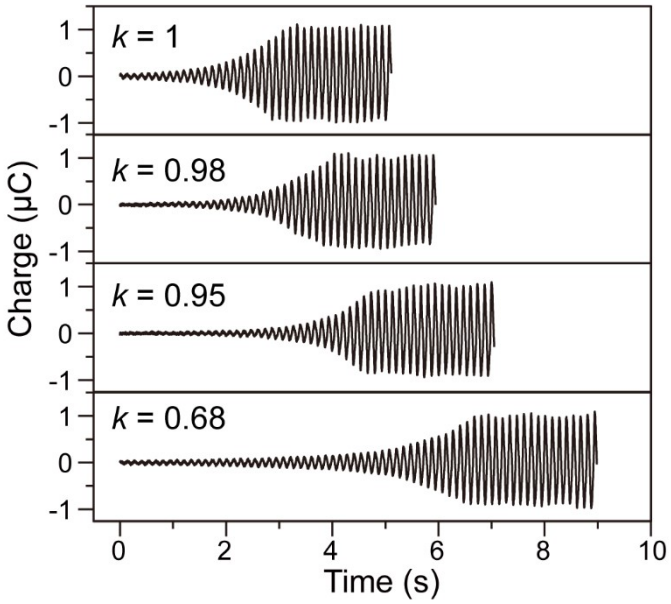

Fig. S6 Comparison of charge outputs under different confinement stiffnesses.

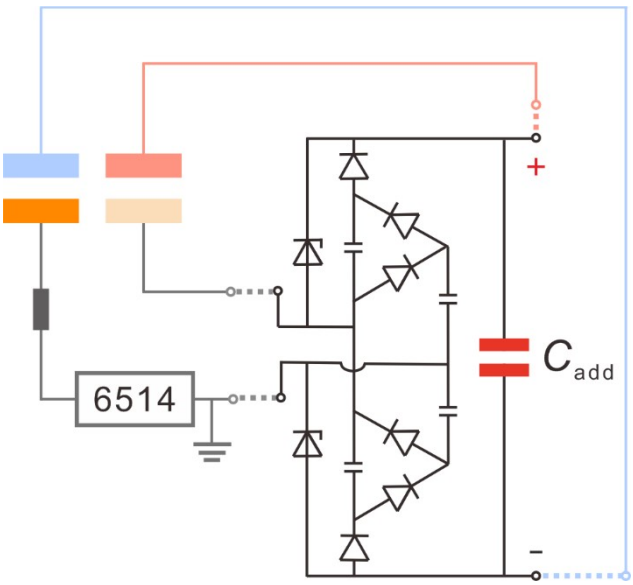

Fig. S7 Test circuit diagram with an additional capacitor (C_{add}).

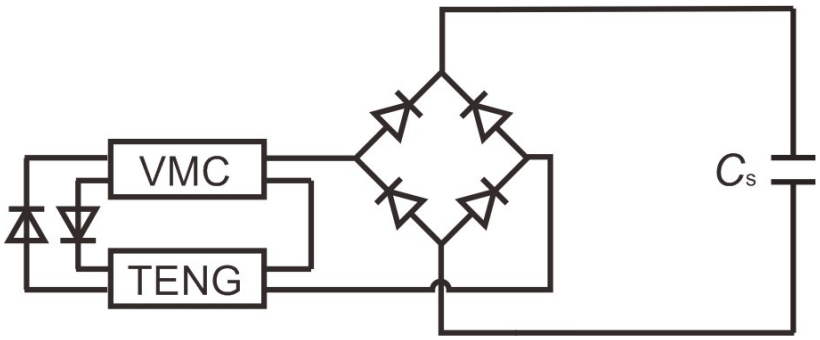

Fig. S8 Circuit diagram for charging the capacitor directly.

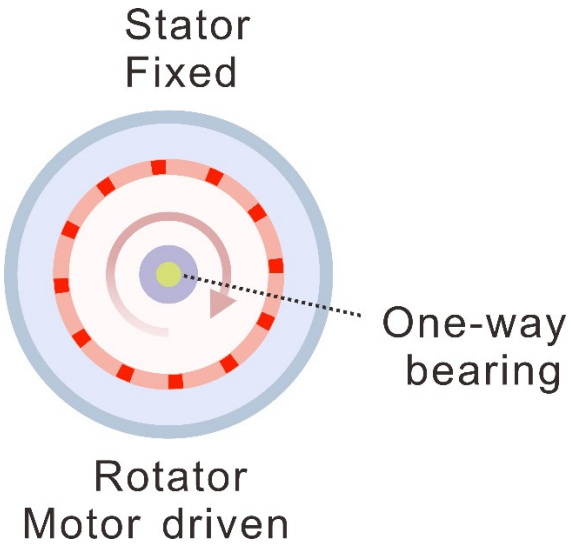

Fig. S9 Schematic illustration of agitating the device with a motor.

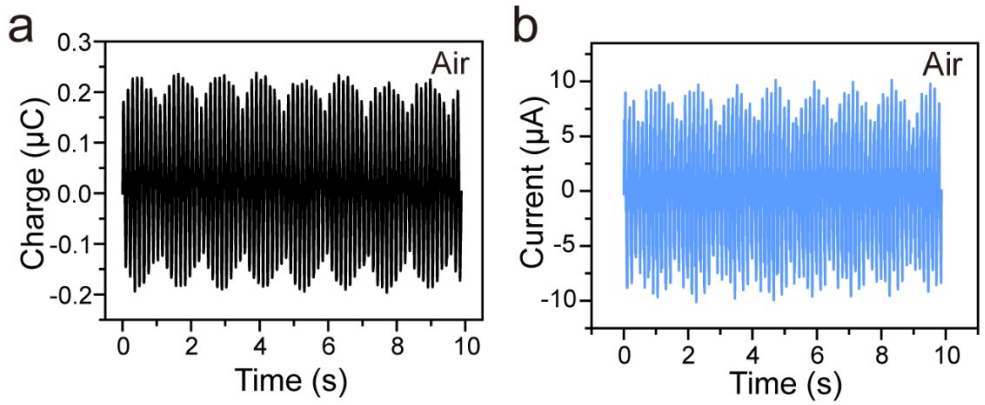

Fig. S10 Transferred charges (a) and current (b) of the device under an agitation speed of 50 rpm in air dielectric.

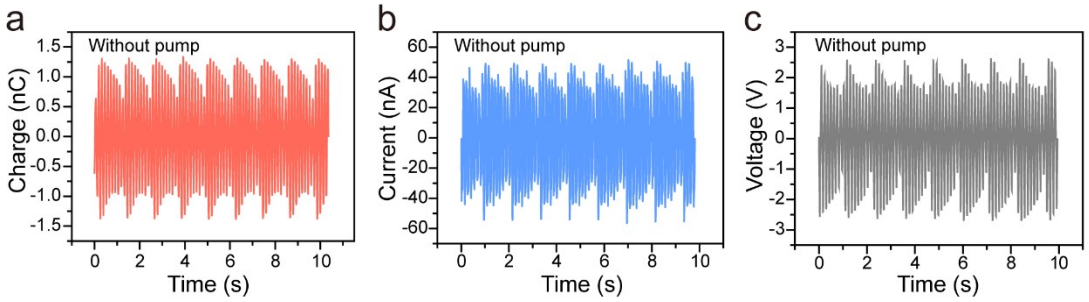

Fig. S11 Transferred charges (a), current (b) and voltage (c) without pump under an agitation speed of 50 rpm in oil dielectric.

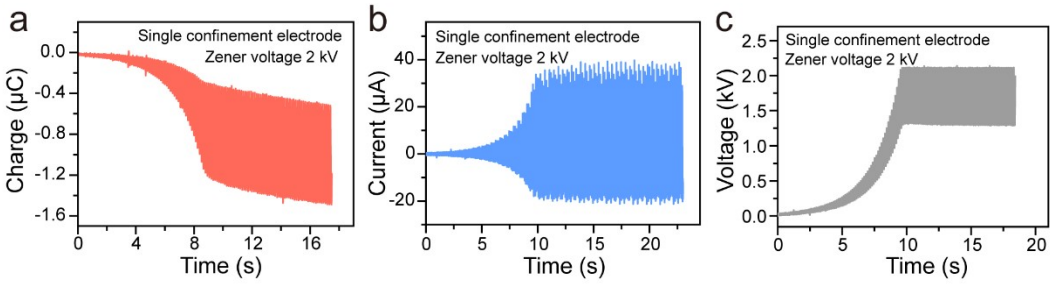

Fig. S12 Transferred charges (a), current (b) and voltage (c) with single CE under an agitation speed of 50 rpm in oil dielectric.

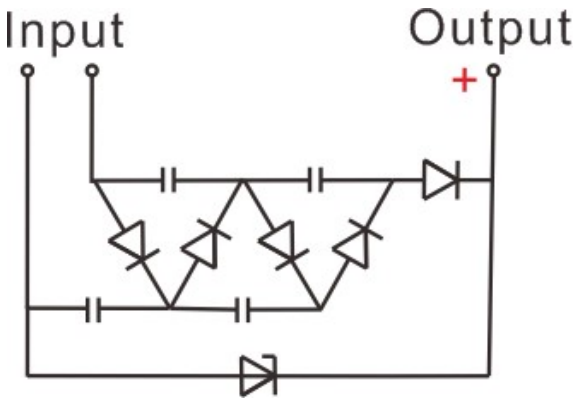

Fig. S13 Scheme of the VMC for single CE.

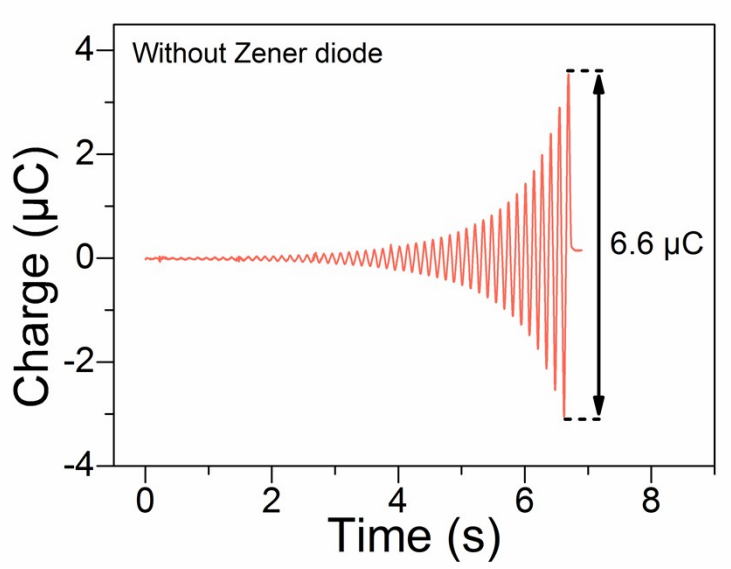

Fig. S14 Charge output without Zener diode under an agitation speed of 50 rpm.

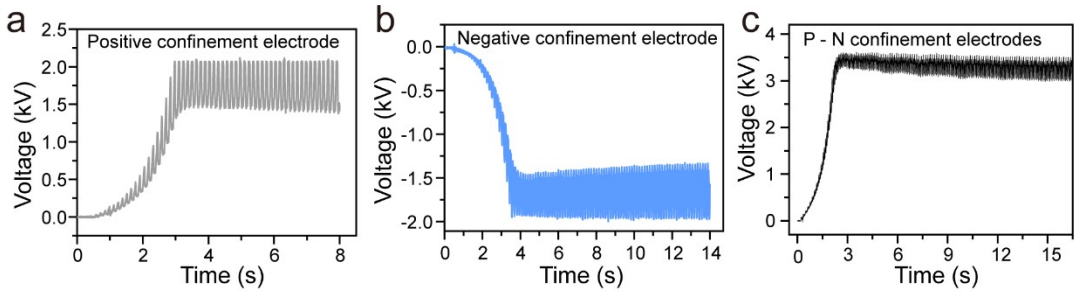

Fig. S15 Voltage on CEs with a 2 kV Zener diode under an agitation speed of 50 rpm. (a) Positive CE. (b) Negative CE. (c) Voltage between positive CE and negative CE.

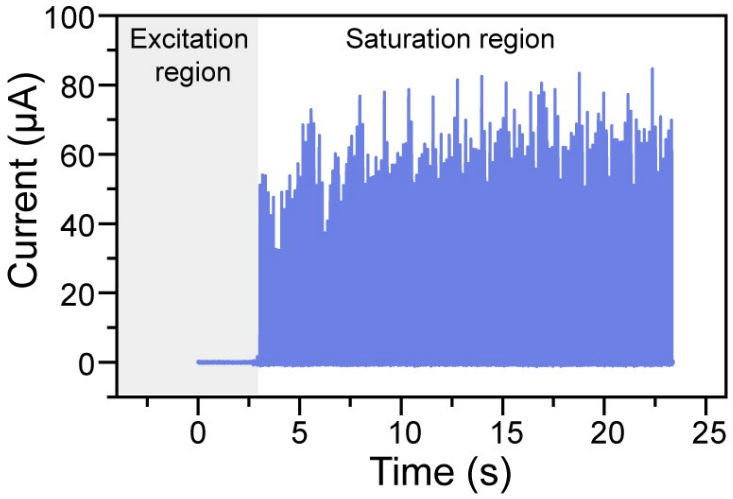

Fig. S16 Current through one Zener diode.

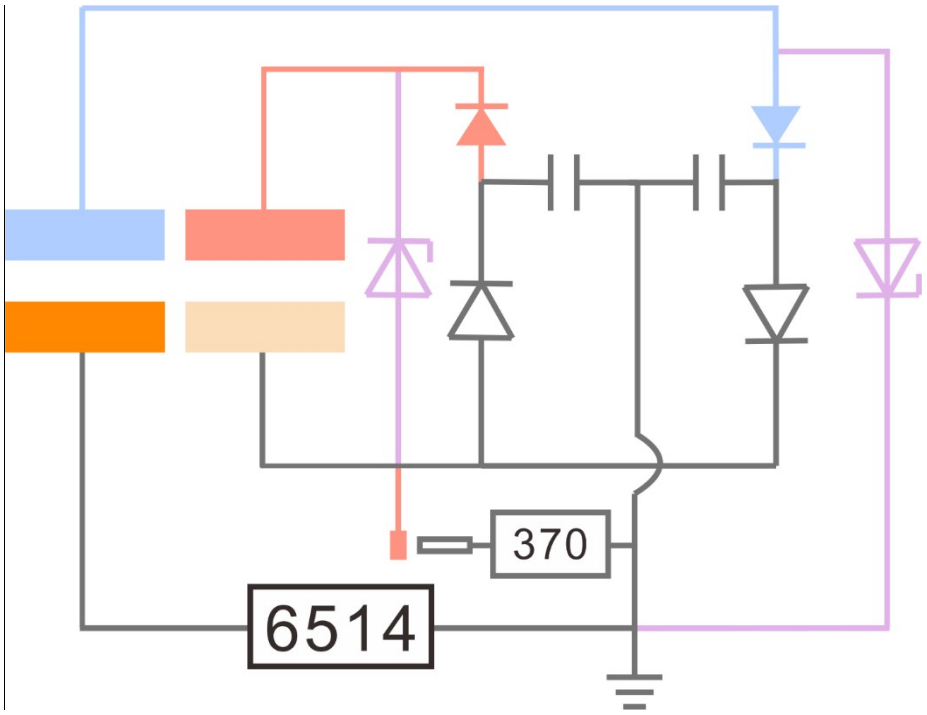

Fig. S17 Schematic diagram on simultaneously measuring the voltage and current of the device, by an electrostatic voltmeter (Trek 370) and an electrometer (Keithley 6514) respectively.

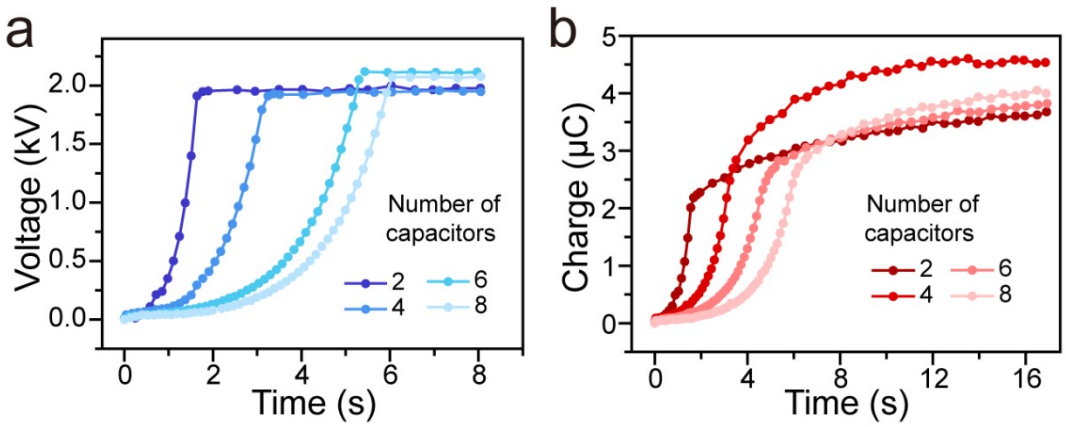

Fig. S18 Voltage of the positive CE (a) and charge output (b) with VMCs using different numbers of capacitors.

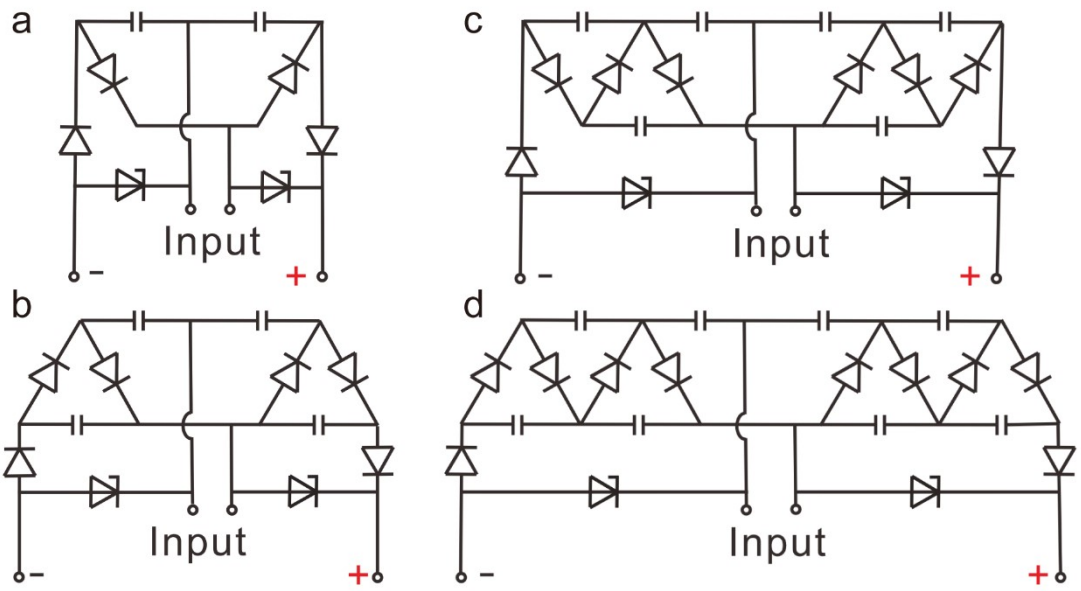

Fig. S19 Circuit diagrams of VMCs using different numbers of capacitors. (a) 2 capacitors. (b) 4 capacitors. (c) 6 capacitors. (d) 8 capacitors.

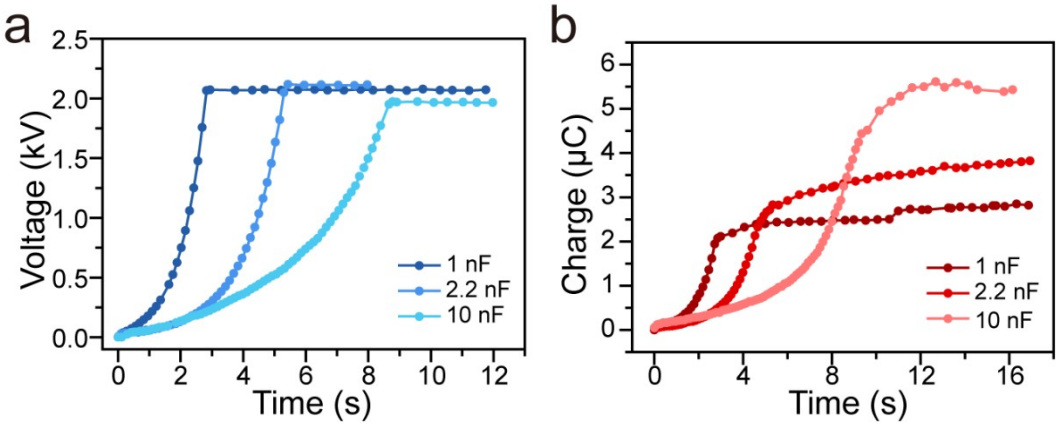

Fig. S20 Voltage of the positive CE (a) and charge output (b) with VMCs using different capacitors.

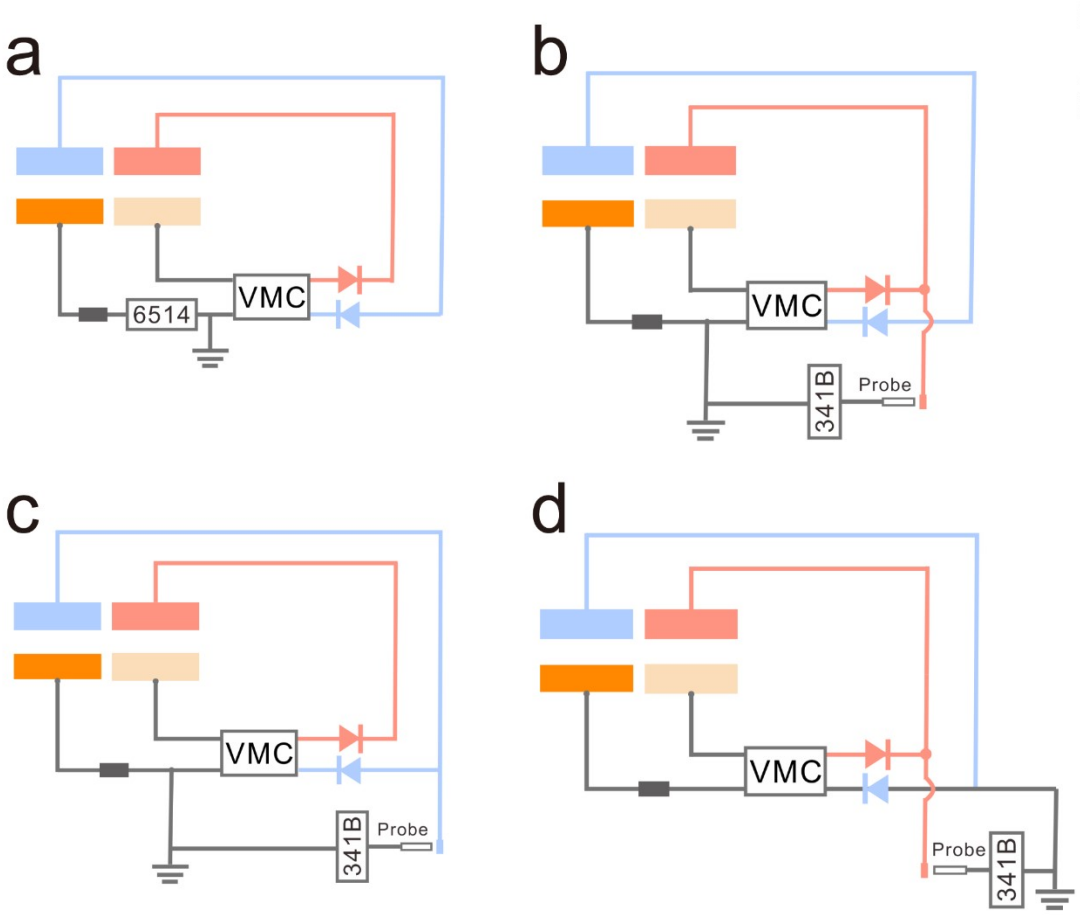

Fig. S21 Circuit diagrams for measuring the output of the device. (a) Measuring the charge and current outputs. (b) Measuring the voltage of the positive CE. (c) Measuring the voltage of the negative CE. (d) Measuring the voltage between the positive CE and negative CE.

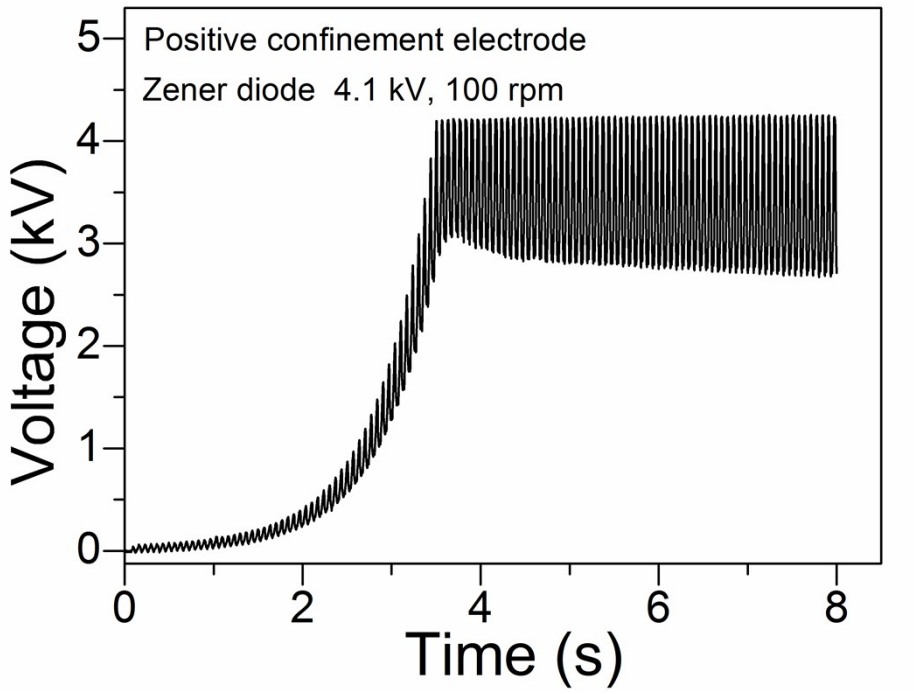

Fig. S22 Voltage of the positive CE with a 4.1 kV Zener diode under an agitation speed of 100 rpm.

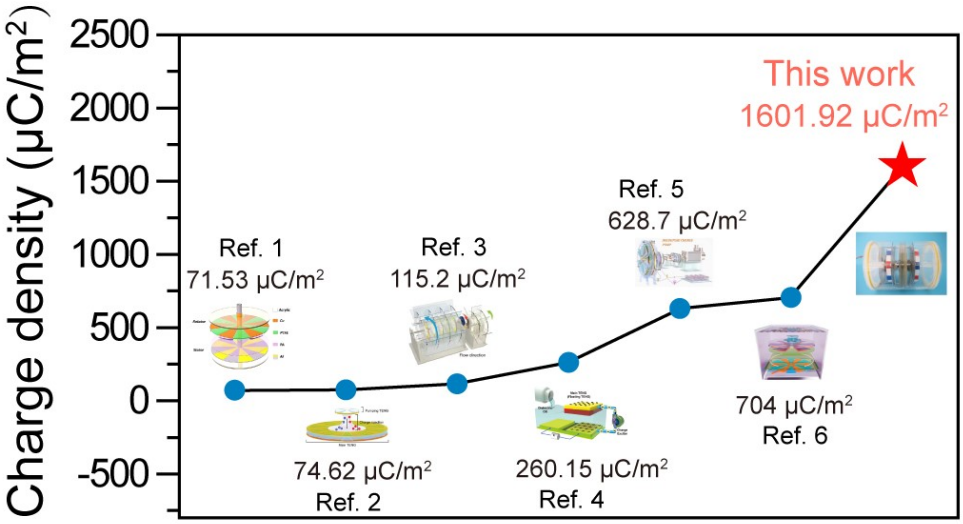

Fig. S23 Comparison of charge density with reported sliding or rotating TENGs.

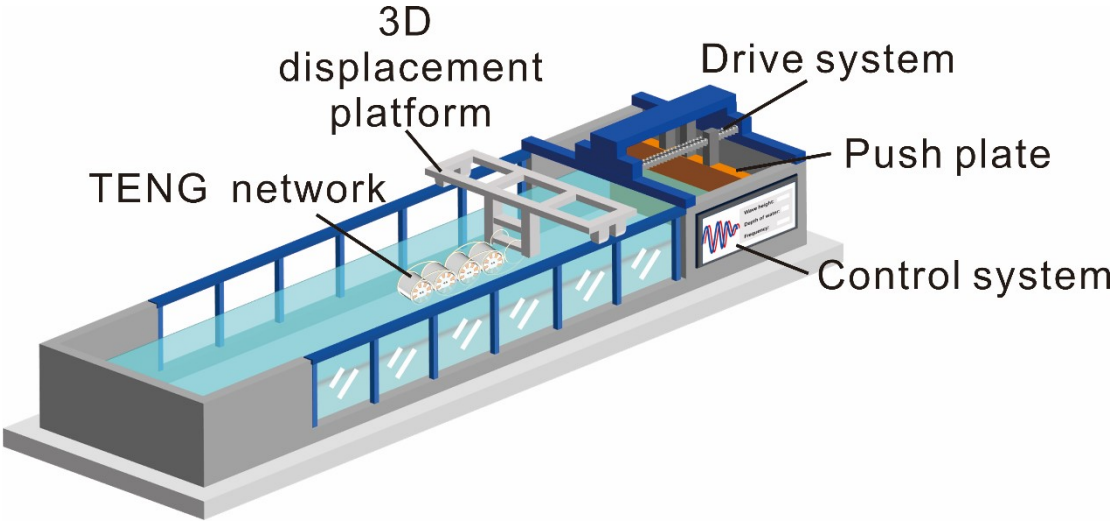

Fig. S24 Schematic structure of the large wave basin.

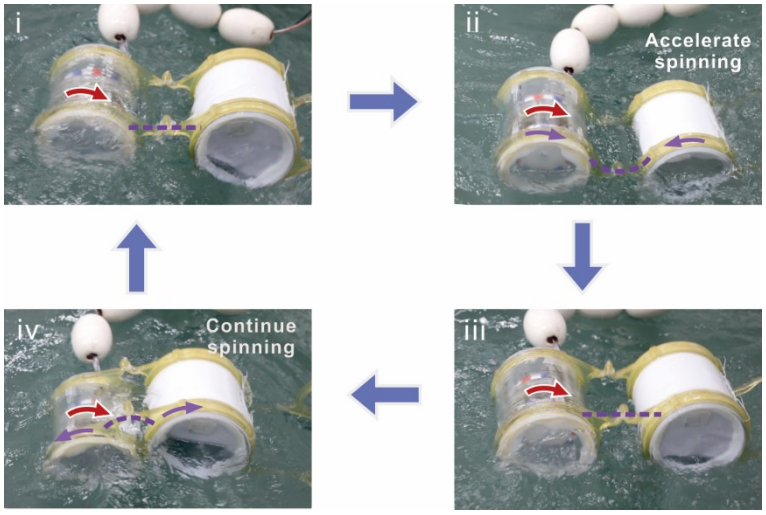

Fig. S25 Photographs on the working process of the device agitated by waves.

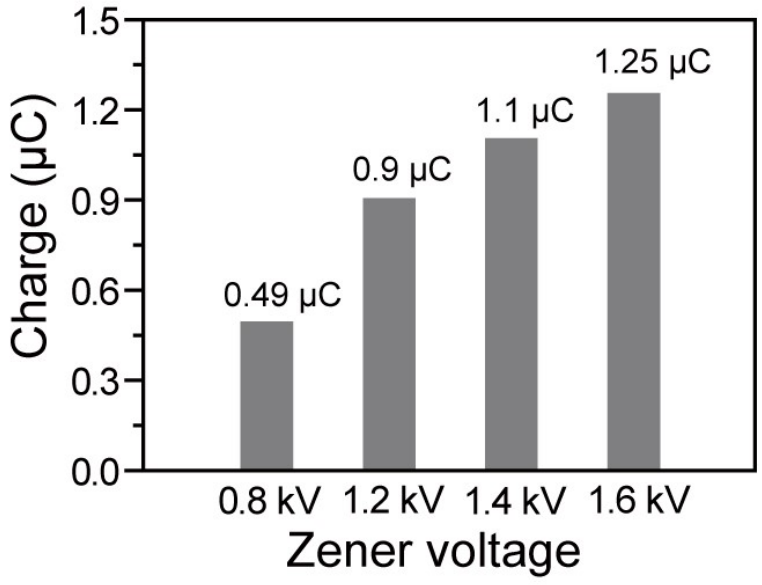

Fig. S26 Charge output of the device with different Zener voltages.

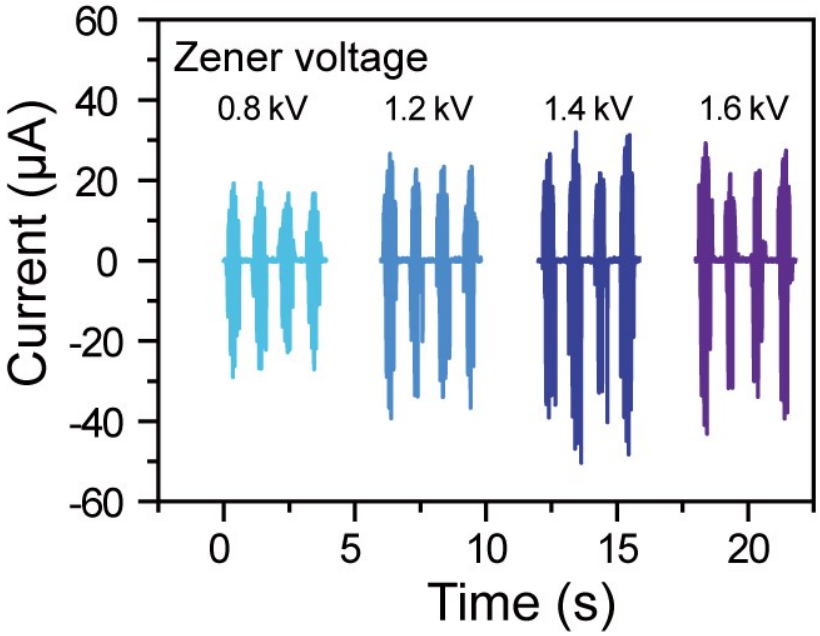

Fig. S27 Current output of the device with different Zener voltages.

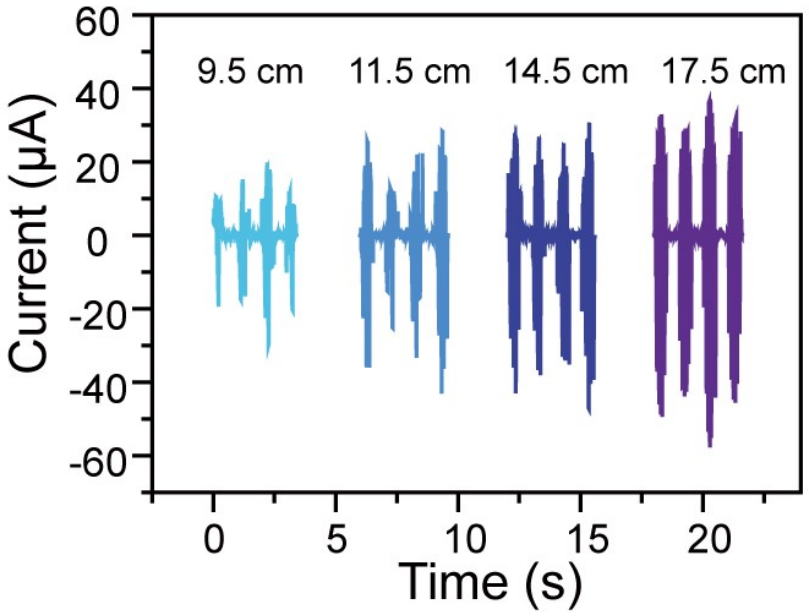

Fig. S28 Current output of the device with different wave heights.

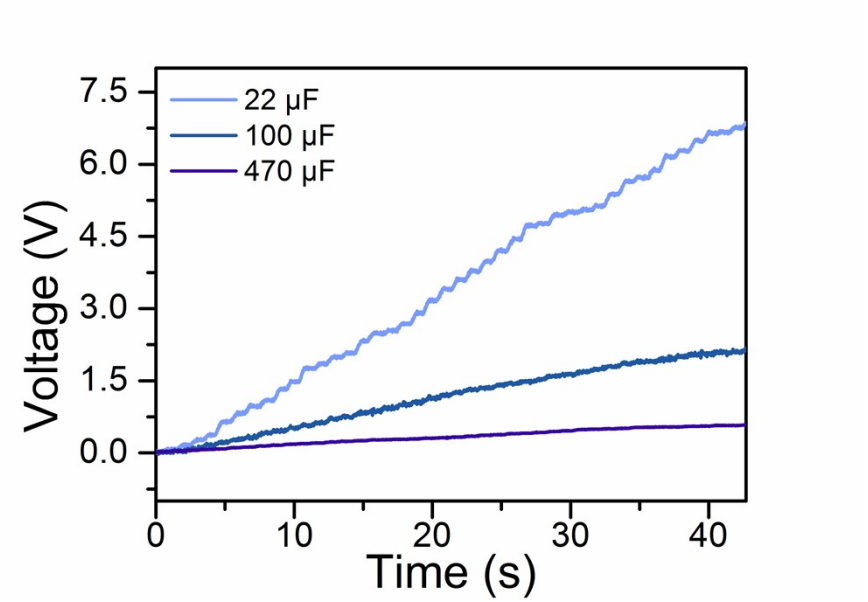

Fig. S29 Charging performance with a full-wave rectifier under a wave height of 17.5 cm.

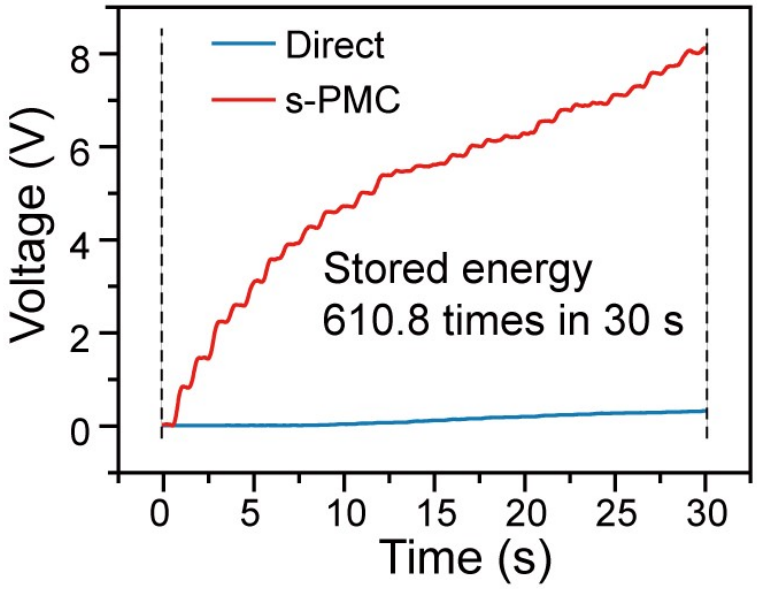

Fig. S30 Comparison of charging performance with and without the s-PMC in water (C_s = 0.47 mF).

References

1. L. Long, W. L. Liu, Z. Wang, W. C. He, G. Li, Q. Tang, H. Y. Guo, X. J. Pu, Y. K. Liu and C. G. Hu, *Nat. Commun.*, 2021, **12**, 4689.

2. S. Lv, H. Li, Y. Xie, B. Zhang, B. Liu, J. Yang, H. Guo, Z. Yang and Z. Lin, *Adv. Energy Mater.*, 2023, **13**, 2301832.

3. P. Chen, J. An, S. Shu, R. Cheng, J. Nie, T. Jiang and Z. L. Wang, *Adv. Energy Mater.*, 2021, **11**, 2003066.

4. R. Lei, S. Li, Y. Shi, P. Yang, X. Tao, H. Zhai, Z. L. Wang and X. Chen, *Adv. Energy Mater.*, 2022, **12**, 2201708.

5. Z. Yang, Y. Yang, F. Liu, B. Li, Y. Li, X. Liu, J. Chen, C. Wang, L. Ji, Z. L. Wang and J. Cheng, *Nano Energy*, 2022, **98**, 107264.

6. W. He, C. Shan, S. Fu, H. Wu, J. Wang, Q. Mu, G. Li and C. Hu, *Adv. Mater.*, 2023, **35**, 2209657.